

Diffractive Higgs production from intrinsic heavy flavors in the protonStanley J. Brodsky,^{1,*} Boris Kopeliovich,^{2,†} Ivan Schmidt,^{2,‡} and Jacques Soffer^{3,§}¹Stanford Linear Accelerator Center, Stanford University, Stanford, California 94309, USA²Departamento de Física, Universidad Técnica Federico Santa María, Casilla 110-V, Valparaíso, Chile³Centre de Physique Théorique, UMR 6207^{||}, CNRS-Luminy Case 907, F-13288 Marseille Cedex 9, France

(Received 29 March 2006; published 19 June 2006)

We propose a novel mechanism for exclusive diffractive Higgs production $pp \rightarrow pHp$ in which the Higgs boson carries a significant fraction of the projectile proton momentum. This mechanism will provide a clear experimental signal for Higgs production due to the small background in this kinematic region. The key assumption underlying our analysis is the presence of intrinsic heavy flavor components of the proton bound state, whose existence at the high light-cone momentum fraction x has growing experimental and theoretical support. We also discuss the implications of this picture for exclusive diffractive quarkonium and other channels.

DOI: [10.1103/PhysRevD.73.113005](https://doi.org/10.1103/PhysRevD.73.113005)

PACS numbers: 14.80.Bn, 12.38.Bx

I. INTRODUCTION

A central goal of the Large Hadron Collider (LHC) being built at CERN is the discovery of the Higgs boson, a key component of the standard model, whose discovery would constitute the first observation of an elementary scalar field. A number of theoretical analyses suggest the existence of a light Higgs boson with a mass $M_H \lesssim 130$ GeV.

In this paper we propose a novel mechanism for hadronic Higgs production, in which the Higgs is produced with a significant fraction of the projectile momentum. The key assumption underlying our analysis is the presence of intrinsic charm (IC) and intrinsic bottom (IB) fluctuations in the proton bound state [1,2], whose existence at high x as large as $x \simeq 0.4$ has substantial and growing experimental and theoretical support. Clearly, this phenomenon can be extended to the consideration of intrinsic top (IT). A recent review of the theory and experimental constraints on the charm quark distribution $c(x, Q^2)$ and its consequences for open and hidden charm production has been given by Pumplin [3]. The presence of high x intrinsic heavy quark components in the proton's structure function will lead to Higgs production at high x_F through subprocesses such as $gb \rightarrow Hb$; such reactions could be particularly important in minimal supersymmetric standard model (MSSM) models in which the Higgs has enhanced couplings to the b quark [4].

The virtual Fock state $|uudQ\bar{Q}\rangle$ of a proton has a long lifetime at high energies and can be materialized in a

collision by the exchange of gluons. The heavy quark and antiquark can then coalesce to produce the Higgs boson at large $x_F \simeq x_c + x_{\bar{c}}$. This Higgs production process can be inclusive as in $pp \rightarrow HX$, semidiffractive $pp \rightarrow HpX$, where one of the projectile protons remains intact, or exclusive diffractive $pp \rightarrow pHp$, where the Higgs can be reconstructed from the missing mass distribution. In each case the Higgs distribution can extend to momentum fractions x_F as large as 0.8, reflecting the combined momentum fractions of the heavy intrinsic quarks.

Perhaps the most novel production process for the Higgs is the exclusive diffractive reaction, $pp \rightarrow p + H + p$ [5], where the $+$ sign stands for a large rapidity gap (LRG) between the produced particles. If both protons are detected, the mass and momentum distribution of the Higgs can be determined. The TOTEM detector [6] proposed for the LHC will have the capability to detect exclusive diffractive channels. The detection of the Higgs via the exclusive diffractive process $pp \rightarrow p + H + p$ has the advantage that it does not depend on a specific decay mechanism for the Higgs. The branching ratios for the decay modes of the Higgs can then be individually determined by combining the measurement of $\sigma(pp \rightarrow p + H + p)$ with the rate for a specific diffractive final state $B_f \sigma(pp \rightarrow p + H_{\rightarrow f} + p)$. This is in contrast to the standard inclusive measurement, where one can only determine the product of the cross section and branching ratios $B_f \sigma(pp \rightarrow H_{\rightarrow f} X)$.

The existing theoretical estimates for diffractive Higgs production are based on the gluon-gluon fusion subprocess, where two hard gluons couple to the Higgs ($gg \rightarrow H$) [5]. A third gluon is also exchanged in order that both projectiles remain color singlets. Perturbative QCD then predicts $\sigma(pp \rightarrow p + H + p) \simeq 3$ fb for the production of a Higgs boson of mass 120 GeV at LHC energies, with a factor of 2 uncertainty [5]. Since the annihilating gluons

*Electronic address: sjbth@slac.stanford.edu†Electronic address: bzk@mpi-hd.mpg.de‡Electronic address: ivan.schmidt@usm.cl§Electronic address: soffer@cpt.univ-mrs.fr

||UMR 6207 is Unité Mixte de Recherche du CNRS et des Universités Aix-Marseille I, Aix-Marseille II et de l'Université du Sud Toulon-Var—Laboratoire affilié à la FRUMAM.

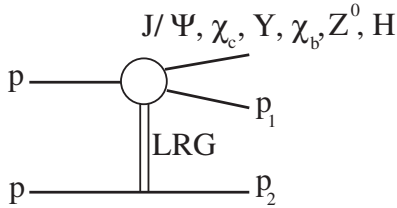


FIG. 1. The exclusive diffractive production of J/ψ , χ_c , Y , χ_b , Z^0 , or H , the standard model Higgs.

each carry a small fraction of the momentum of the proton, the Higgs is primarily produced in the central rapidity region.

In this paper we will specifically consider the exclusive diffractive production reaction $pp \rightarrow pM + p$, depicted in Fig. 1, where M stands for J/ψ , χ_c , Y , χ_b , Z^0 , or H . The final state M will be produced in the projectile proton's fragmentation region with a significant fraction x_F of the incident proton's momentum, since the sum of the momenta of two heavy quarks contributes to the momentum of M . This has an important advantage of providing a distinctive signal with relatively small background. This production process is analogous to the positron-antiproton coalescence reaction by which antihydrogen was first detected [7–9].

II. INTRINSIC HEAVY QUARKS

The proton eigenstate $|p\rangle = \sum_{n=3} \psi_n(x_i, \vec{k}_{\perp i}, \lambda_i) \times |n; x_i, \vec{k}_{\perp i}, \lambda_i\rangle$ of the QCD light-front Hamiltonian $H_{\text{LF}}^{\text{QCD}}$ can be expanded at fixed light-front time $\tau = t + z/c$ as a superposition of quark and gluon Fock eigenstates of the free Hamiltonian H_{LF}^0 : $|p\rangle = |uud\rangle, |uudg\rangle, \dots$, including, in particular, a “hidden charm” Fock component $|uudc\bar{c}\rangle$. The fact that the hadronic eigenstate has fluctuations with an arbitrary number of constituents is a consequence of quantum mechanics and relativity. The $|uudc\bar{c}\rangle$ Fock state arises in QCD not only from gluon splitting which is included in DGLAP evolution, but also from diagrams in which the heavy quark pair is multiconnected to the valence constituents. The latter components are called “intrinsic charm” Fock components. The frame-independent light-front wave functions $\psi_n(x_i, \vec{k}_{\perp i}, \lambda_i)$ describe the constituents in the hadron with momenta $p_i^+ = x_i P^+$, $\vec{p}_{\perp i} = x_i \vec{P}_{\perp} + \vec{k}_{\perp i}$ and spin projection λ_i . Here $\sum_{i=1}^n x_i = 1$, and $\sum_{i=1}^n \vec{k}_{\perp i} = \vec{0}$. The light-cone momentum fractions $x_i = p_i^+ / P^+ = (p_i^0 + p_i^z) / (P^0 + P^z)$ are boost invariant [10].

It was originally suggested in Refs. [1,2] that there is a $\sim 1\%$ probability of IC Fock states in the nucleon; more recently, the operator product expansion has been used to show that the probability for Fock states in the light hadron to have an extra heavy quark pair of mass M_Q decreases only as $\Lambda_{\text{QCD}}^2 / M_Q^2$ in non-Abelian gauge theory [11]. In contrast, in the case of Abelian QED, the probability of an

intrinsic heavy lepton pair in a light atom such as positronium is suppressed by $\mu_{\text{Bohr}}^4 / M_\ell^4$, where μ_{Bohr} is the Bohr momentum. The quadratic QED scaling corresponds to the dimension-8 Euler-Heisenberg effective Hamiltonian F^4 / M_ℓ^4 for light-by-light scattering mediated by heavy leptons. Here $F_{\mu\nu}$ is the electromagnetic field strength. In contrast, the corresponding effective Hamiltonian in QCD G^3 / M_Q^2 has dimension 6. This difference in power behavior provides a remarkable discriminant between non-Abelian and Abelian theory.

The maximal probability for an intrinsic heavy quark Fock state occurs for minimal off-shellness, i.e., at minimum invariant mass squared $\mathcal{M}^2 = \sum_{i=3}^n (m_i^2 + \vec{k}_{\perp i}^2) / x_i$. Thus the dominant Fock state configuration is $x_i \propto m_{\perp i}^2$ where $m_{\perp i}^2 = m_i^2 + \vec{k}_{\perp i}^2$, i.e., at equal rapidity. Since all of the quarks tend to travel coherently at the same rapidity in the $|uudQ\bar{Q}\rangle$ intrinsic heavy quark Fock state, the heaviest constituents carry the largest momentum fraction [1,2]. Models for the intrinsic heavy quark distributions $c_f(x, Q^2)$ and $b_f(x, Q^2)$ predict a peak at $x \sim 0.4$. Thus the intrinsic heavy quarks are highly efficient carriers of the projectile momentum.

Intrinsic charm also leads to new, competitive decay mechanisms for B decays which are Cabibbo-Kobayashi-Maskawa suppressed [12], and to an explanation of the $J/\psi \rightarrow \rho\pi$ puzzle [13]. Furthermore, it has been found that the intrinsic bottom could even contribute significantly to exotic processes such as neutrinoless $\mu^- - e^-$ conversion in nuclei [14].

III. RELEVANT EXPERIMENTAL FACTS

The most direct test of intrinsic charm is the measurement of the charm quark distribution $c(x, Q^2)$ in deep inelastic lepton-proton scattering $\ell p \rightarrow \ell' c X$. The only experiment which has looked for a charm signal in the large x_{Bj} domain is the European Muon Collaboration (EMC) experiment [15], which used prompt muon decay in deep inelastic muon-proton scattering to tag the produced charm quark. The EMC data show a distinct excess of events in the charm quark distribution at $x_{\text{Bj}} > 0.3$, at a rate at least an order of magnitude beyond predictions based on gluon splitting and DGLAP evolution. Next-to-leading-order (NLO) analyses [16] show that an intrinsic charm component, with probability of order 1%, is needed to fit the EMC data in the large x_{Bj} region. This value is consistent with an estimate based on the operator product expansion [11]. Clearly it would be very valuable to have additional direct measurements of the charm and bottom structure functions at large x .

An immediate consequence of intrinsic charm is the production of charmonium states at high $x_F = x_c + x_{\bar{c}}$ in high energy hadronic collisions such as $pp \rightarrow J/\psi X$. The c and \bar{c} in the IC Fock state $|uudc\bar{c}\rangle$ can be materialized by gluon exchange as a color-singlet pair which coalesces to a

high x_F low p_T quarkonium state. The internal color structure of the Fock state is important. The effective operator in the non-Abelian theory predicts that the charm quark pair is dominantly a color octet 8_C . The color octet $(c\bar{c})_{8_C}$ is then converted to a high x color-singlet $(c\bar{c})_{1_C}$ state via gluon exchange with the target; it then couples to the color-singlet quarkonium state. Note that the J/ψ can be produced this way only from the component of IC which is symmetric, relative to a simultaneous permutation of spatial and spin variables.

Comprehensive measurements of the $pA \rightarrow J/\psi X$ and $\pi A \rightarrow J/\psi X$ cross sections have been performed by fixed-target experiments, NA3 at CERN [17] and E886 at FNAL [18]. According to the arguments in Refs. [19–21], the IC contribution is strongly shadowed, thus accounting for the observed nuclear dependence of the high x_F component of the J/ψ hadroproduction. It is also important to consider effects coming from energy conservation. Multiple interactions in a nucleus can resolve higher Fock components of the projectile hadron compared to interaction with a free proton target. Therefore, energy sharing between the projectile partons imposes more severe restrictions on production of energetic particles leading to nuclear suppression at large x_F [22].

The materialization of the intrinsic charm Fock state also leads to the production of open-charm states such as $\Lambda(cud)$ and $D^-(\bar{c}d)$ at large x_F . This may occur either through the coalescence of the valence and charm quarks, which are comoving with the same rapidity, thus producing a leading particle effect, or via hadronization of the produced c and \bar{c} . As shown in Refs. [23,24], a model based on intrinsic charm naturally accounts for the production of leading charm hadrons in $pp \rightarrow DX$ and $pp \rightarrow \Lambda_c X$ as observed at the ISR [25] and also at Fermilab [26,27]. Additionally, we note that it is also possible to construct Regge models which give similar x_F behavior to the IC approach.

The diffractive cross section $\sigma(pp \rightarrow \Lambda_c X + p)$, at $\sqrt{s} = 63$ GeV, was measured at the ISR to be of order 10 to 60 μb [28]. This result seems to be in contradiction with findings of Fermilab experiments searching for diffractive charm production [29,30]. The E690 experiment [29] observed the diffractive channel $\sigma(pp \rightarrow D^* pX) \sim 0.2 \mu b$ at $\sqrt{s} = 40$ GeV. Their results lead to the diffractive charm production cross section $\sigma_{\text{diff}}(\bar{c}c)^{pp} = 0.6\text{--}0.7 \mu b$ which is about 2 orders of magnitude smaller than the cross section measured at ISR [28]. This result agrees with the upper limit found for coherent diffractive production of charm, $pSi \rightarrow \bar{c}cX + Si$, in the E653 experiment [30] at Fermilab. However, forward charm production is most likely strongly suppressed in a nuclear target as is the case for light hadrons. If one extrapolates to pp collisions assuming an $A^{1/3}$ dependence [31], the upper limit is $\sigma_{\text{diff}}(\bar{c}c)^{pp} < 7 \mu b$. The ISR signals for forward charm production are thus not necessarily inconsistent with

the fixed-target experiments considering the large differences in the available center of mass energy, as well as the nuclear target suppression.

It should be noted that diffractive charm production via elastic scattering of the projectile plus gluon radiation also leads to the right order of magnitude of the cross section. Indeed, the cross section for diffractive gluon radiation (via the triple-Pomeron term) in pp collisions is known from data, $\sigma_{sd}^{3P} \approx 4$ mb. The production of a $\bar{c}c$ pair via a radiated gluon brings extra factors from the coupling $\alpha_s \approx 0.2$ and from the gluon propagator $(m_g/M_{\bar{c}c})^4$ where $m_g \approx 0.8$ GeV is the effective gluon mass [32]. Thus, one obtains an estimate for the singly diffractive charm production cross section $\sigma(pp \rightarrow c\bar{c}pX) \approx 4 \mu b$, in good agreement with the magnitude of the data, at least in the central rapidity region. However, the shape of the empirical Λ_c distribution at large x_F is not readily accounted for in this model.

One can produce the $\Lambda(bud)$ at high x_F in inclusive pp collisions, through the materialization of the intrinsic bottom Fock state $|(uud)_{8_C}(b\bar{b})_{8_C}\rangle$. The cross section for forward open bottom production relative to open charm is reduced by the relative IC/IB probability factor $m_c^2/m_b^2 \sim 1/10$. Evidence for the forward production of the Λ_b in $pp \rightarrow \Lambda_b X$ at the ISR was reported in Ref. [33].

The existence of rare double-IC Fock state fluctuations in the proton, such as $|uudc\bar{c}\bar{c}\rangle$, can lead to the production of two J/ψ 's [34] or a double-charm baryon state at large x_F and small p_T . Double- J/ψ events at a high combined $x_F \geq 0.5$ were, in fact, observed by NA3 [35]. The observation of the doubly charmed baryon $\Xi_{cc}^+(3520)$ with mean $\langle x_F \rangle \approx 0.33$ has been reported by the SELEX Collaboration at FNAL [36]; the presence of two charm quarks at large x_F has, indeed, a natural IC interpretation.

IV. INTRINSIC HEAVY QUARKS AND EXCLUSIVE DIFFRACTIVE PRODUCTION

We now investigate the implications of IC and IB for exclusive diffractive production processes $pp \rightarrow pMp$ at

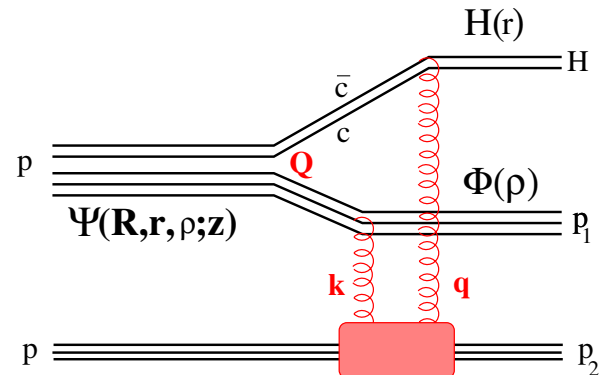


FIG. 2 (color online). The two-gluon exchange diagram for the Higgs exclusive production.

large x_F where M is a charmonium state, a Z^0 boson, or the Higgs. We first explain, using Fig. 2, how the exclusive diffractive channels shown in Fig. 1 arise with the required color structure in the final state. As noted above, we shall assume that the projectile (upper) proton has an approximate 1% probability to fluctuate to an IC Fock component with the color structure $[[uud]_{8_c}[\bar{c}c]_{8_c}]$. This virtual state has a long coherence length in a high energy collision $\propto s/\mathcal{M}^2 M_p$, where \mathcal{M} is the total invariant final-state mass. In a pp collision, two soft gluons must be exchanged in order to keep both protons intact and to create a rapidity gap, mimicking Pomeron exchange. The two gluons couple the target nucleon to the large color dipole moment of the projectile IC Fock state. For example, as shown in Fig. 2, one of the exchanged gluons can be attached to the d valence quark spectator in $[[uud]_{8_c}[\bar{c}c]_{8_c}]$, changing its color, and the other one can be attached to the \bar{c} , also changing its color. The net effect of this color rearrangement is the same as single-gluon exchange between the two color-octet clusters. The $\bar{c}c$ and the uud can thus emerge as color singlets because of the gluonic exchange. The $[\bar{c}c]_{1_c}$ can couple to the J/ψ , or to a Z^0 or an H . Meanwhile the color singlet uud gives rise to the scattered proton, thus producing the two required rapidity gaps in the final state. Notice that the x_F distribution of the produced particle is approximately the same as the distribution of the $[\bar{c}c]$ inside the proton. As we shall discuss below, the sum of couplings of the gluon to all of the quarks, as dictated by gauge invariance, brings in a form factor which vanishes at zero momentum transfer, thus giving an important suppression factor.

A. The cross section

The cross section of exclusive diffractive production of the Higgs, $pp \rightarrow Hp + p$, can be estimated in the light-cone (LC) dipole approach [37]. The Born graph for this process is shown in Fig. 2. As discussed above, we shall assume the presence in the proton of an IC component, a $\bar{c}c$ pair, which is predominantly in a color-octet state, and which has either a nonperturbative or perturbative origin. In the former case this heavy component can interact strongly with the $3q$ valence quark component. Such non-perturbative reinteractions of the intrinsic sea quarks in the proton wave function can lead to a $Q(x) \neq \bar{Q}(x)$ asymmetry as in the ΛK model for the $s\bar{s}$ asymmetry [38,39]. As in the charmonium, the mean $\bar{c}c$ separation should be considerably larger than the transverse size $1/m_c$ of perturbative $\bar{c}c$ fluctuations. For instance, if the binding potential

has the oscillator form, the mean distance is

$$\langle r_{\bar{c}c}^2 \rangle = \frac{2}{\omega m_c}, \quad (1)$$

where $\omega \sim 300$ MeV is the oscillation frequency. Alternatively, the IC component can be considered to derive perturbatively from the minimal gluonic couplings of the heavy quark pair to two valence quarks of the proton; this is likely the dominant mechanism at the largest values of x_c [21]. In this case the transverse separation of the $\bar{c}c$ is controlled by the energy denominator, $\langle r_{\bar{c}c}^2 \rangle = 1/m_c^2$, and is much smaller than the estimate given by Eq. (1).

In accordance with the notation in Fig. 2 the two protons in the center of mass frame are detected with Feynman momentum fractions x_1 and x_2 and transverse momenta \vec{p}_1 and \vec{p}_2 , respectively. Correspondingly, the produced Higgs carries longitudinal momentum $(x_2 - x_1)$ and transverse momentum $\vec{p}_H = -(\vec{p}_1 + \vec{p}_2)$. We assume the Higgs to be heavy, over 100 GeV; then x_1 and x_2 turn out to be tightly correlated in this reaction. Indeed, the effective mass squared of the $H - p_1$ pair reads

$$M^2 = \frac{M_H^2 + \vec{p}_H^2}{1 - x_1} + \frac{m_p^2 + \vec{p}_1^2}{x_1} - \vec{p}_2^2. \quad (2)$$

(We assume the equivalence of Feynman x and the corresponding fractions of the light-cone momenta, which is an accurate approximation at large x .) Because of the form factors of the two protons, neither transverse momenta, $\vec{p}_{1,2}$, can be much larger than a few hundred MeV and therefore they, together with \vec{p}_H and the proton mass, can be safely neglected in Eq. (2). This could be incorrect at very small values of $x_1 \sim m_p^2/M_H^2$, but we will show that the x_1 distribution sharply peaks at $\bar{x}_1 \approx 0.25$. Then, employing the standard relation $M^2/s = 1 - x_2$, we arrive at the simple relation

$$(1 - x_1)(1 - x_2) = \frac{M_H^2}{s}. \quad (3)$$

The diffractive cross section has the form

$$\frac{d\sigma(pp \rightarrow ppH)}{dx_2 d^2 p_1 d^2 p_2} = \frac{1}{(1 - x_2)16\pi^2} |A(x_2, \vec{p}_1, \vec{p}_2)|^2, \quad (4)$$

where the diffractive amplitude in Born approximation reads

$$A(x_2, \vec{p}_1, \vec{p}_2) = \frac{8}{3\sqrt{2}} \int d^2 Q \frac{d^2 q}{q^2} \frac{d^2 k}{k^2} \alpha_s(q^2) \alpha_s(k^2) \delta(\vec{q} + \vec{p}_2 + \vec{k}) \delta(\vec{k} - \vec{p}_1 - \vec{Q}) \int d^2 \tau |\Phi_p(\tau)|^2 [e^{i(\vec{k} + \vec{q}) \cdot \vec{\tau}/2} - e^{i(\vec{q} - \vec{k}) \cdot \vec{\tau}/2}] \\ \times \int d^2 R d^2 r d^2 \rho H^\dagger(\vec{r}) e^{i\vec{q} \cdot \vec{r}/2} (1 - e^{-i\vec{q} \cdot \vec{r}}) \Phi_p^\dagger(\vec{\rho}) e^{i\vec{k} \cdot \vec{\rho}/2} (1 - e^{-i\vec{k} \cdot \vec{\rho}}) \Psi_p(\vec{R}, \vec{r}, \vec{\rho}, z) e^{i\vec{Q} \cdot \vec{R}}. \quad (5)$$

Here $\Psi_p(\vec{R}, \vec{r}, \vec{\rho}, z)$ is the light-cone wave function of the IC component of the projectile proton with transverse separations \vec{R} between the $\bar{c}c$ and $3q$ clusters, \vec{r} between the c and \bar{c} , \vec{Q} is the relative transverse momentum of the $3q$ and $\bar{c}c$ clusters in the projectile, and $\vec{\rho}$ is the transverse separation of the quark and diquark which couple to the final-state proton p_2 . The density $|\Phi_p(\tau)|^2$ is the wave function of the target proton which we also treat as a color dipole quark-diquark with transverse separation τ . (The extension to three quarks is straightforward [37].) The fraction of the projectile proton light-cone momentum carried by the $\bar{c}c$ is $z \approx 1 - x_1$. This wave function is normalized as

$$\int_0^1 dz \int d^2R d^2r d^2\rho |\Psi_p(\vec{R}, \vec{r}, \vec{\rho}, z)|^2 = P_{\text{IC}}, \quad (6)$$

where P_{IC} is the weight of the IC component of the proton, which is suppressed as $1/m_c^2$, and is assumed to be $P_{\text{IC}} \sim 1\%$. The amplitudes $H(\vec{r})$ and $\Phi_p(\vec{\rho})$ denote the wave functions of the produced Higgs and the outgoing proton, respectively, in accordance with Fig. 2.

The phase factors in Eq. (5) correspond to different attachments of the exchanged gluons to quarks in Fig. 2. Thus, attaching the gluon either to the c or to the \bar{c} quarks one gets the factor $[\exp(i\vec{q} \cdot \vec{r}/2) - \exp(-i\vec{q} \cdot \vec{r}/2)]$. An analogous factor corresponding to the second gluon coupling to the proton p_1 is also included in Eq. (5). The transverse coordinates of the quark and diquark in the target proton are $\tau/2$ and $-\tau/2$ (relative to its center of gravity). The phase factor in the square brackets in Eq. (5) thus includes two terms corresponding to attachment of the exchanged gluons to the same or different valence quark or diquark in p_2 .

Notice that, in our QCD mechanism for high x_F exclusive Higgs production $pp \rightarrow pHp$, there is no Sudakov suppression. Although we have a large rapidity gap (LRG) process, not every LRG is associated with a Sudakov suppression. For instance, elastic scattering, which is a shadow of all inelastic processes, has no Sudakov factor. On the other hand, the inelastic diffraction amplitude is a linear superposition of elastic amplitudes [40]. Therefore, it should not have any Sudakov factor either.

Furthermore, the incoming IC Fock state, when it appears, is already in the needed color coherent and rapidity configuration to produce the forward diffractive state from two-gluon exchange. Since we fit the required dipole cross section to the diffractive deep inelastic scattering data, our phenomenological Pomeron includes the relevant evolution and suppression effects.

In order to advance the calculations further, we will take the following steps: first, we assume a factorized form of the proton wave function,

$$\Psi_p(\vec{R}, \vec{r}, \vec{\rho}, z) = \Psi_{\text{IC}}(\vec{R}, z) \Psi_{\bar{c}c}(\vec{r}) \Psi_{3q}(\vec{\rho}). \quad (7)$$

Here $\Psi_{\bar{c}c}$ and Ψ_{3q} are the $\bar{c}c$ and $3q$ wave functions

normalized to unity, whereas $\Psi_{\text{IC}}(\vec{R}, z)$ is the wave function describing the relative motion of the $\bar{c}c$ and $3q$ clusters, where z is the fraction of the longitudinal momentum carried by the $\bar{c}c$. This wave function is normalized as

$$\int d^2R |\Psi_{\text{IC}}(\vec{R}, z)|^2 = P_{\text{IC}}(z), \quad (8)$$

where $P_{\text{IC}}(z)$ is the z distribution of $\bar{c}c$, related to the x_1 distribution of the produced protons, since with a very high precision $z = 1 - x_1 = M_H^2/s(1 - x_2)$ (unless x_1 is as small as $x_1 \sim 2m_p/\sqrt{s}$).

We will perform the calculations in Eq. (5) only for forward diffraction, i.e. $p_2 = 0$, $\vec{q} = -\vec{k}$, and we assume for the Pomeron the typical Gaussian t dependence ($t = -p_2^2$),

$$\frac{d\sigma}{d^2p_1 d^2p_2} \propto e^{-B(s')p_2^2}, \quad (9)$$

so the t -integrated cross section then reads

$$\frac{d\sigma}{d^2p_1 dx_2} = \frac{\pi}{B(s')} \frac{d\sigma}{d^2p_1 d^2p_2 dx_2} \Big|_{p_2=0}. \quad (10)$$

Here the slope $B(s') \sim B_0 + 2\alpha'_p \ln(s'/M_0^2)$, where $B_0 = 4 \text{ GeV}^{-2}$, $\alpha'_p = 0.25 \text{ GeV}^{-2}$, $s'/M_0^2 = s/M_H^2$, and $M_0 = 1 \text{ GeV}$.

The next step is to replace the two-gluon proton vertex, represented by the integral over $\vec{\tau}$ in Eq. (5), by the unintegrated gluon density, $\mathcal{F}(x, k^2) = \partial G(x, k^2)/\partial(\ln k^2)$, where $G(x, Q^2) = xg(x, Q^2)$. This preserves the infrared stability of the cross section, since \mathcal{F} vanishes at $k^2 \rightarrow 0$. The phenomenological gluon density fitted to data includes by default all higher order corrections and supplies the cross section with an energy dependence important for extrapolation to very high energies. One can relate the unintegrated gluon distribution to the phenomenological dipole cross section fitted to data for $F_2(x, Q^2)$ from HERA, as was done in Ref. [41],

$$\mathcal{F}(x, k^2) = \frac{3\sigma_0}{16\pi^2\alpha_s(k^2)} k^4 R_0^2(x) \exp\left[-\frac{1}{4}R_0^2(x)k^2\right]. \quad (11)$$

The problem is the extrapolation to the small virtualities k^2 typical for the process under consideration. The Bjorken variable is not a proper variable for soft reactions; therefore we use the parametrization from Ref. [32] adjusted to data for soft interactions. Then $R_0(x)$ in Eq. (11) should be replaced by $R_0(s') = 0.88 \text{ fm} \times (s'/s_0)^{-\lambda/2}$ with $\lambda = 0.28$, $s_0 = 1000 \text{ GeV}^2$, and $\sigma_0 \Rightarrow \sigma_0(s') = \sigma_{\text{tot}}^{\pi p}(s') \times [1 + 3R_0^2(s')/8\langle r_{\text{ch}}^2 \rangle \pi]$, where $\sigma_{\text{tot}}^{\pi p}(s') = 23.6 \text{ mb} \times (s'/s_0)^{0.08}$ is the Pomeron part of the πp total cross section. The energy variable s' is related to the rapidity gap between the two protons in the final state, controlled by x_2 ,

$$s' = \frac{M_0^2}{1 - x_2} = s(1 - x_1) \frac{M_0^2}{M_H^2}. \quad (12)$$

At the energy of the LHC, the longitudinal momentum transfer is very small, even for Higgs production, since $q_L = (M_H^2/s)m_N$; therefore the skewness effect for the unintegrated gluon distributions can be safely neglected. One can check this point using data for the photoproduction of the J/ψ at HERA, which has approximately the

$$\frac{d\sigma^{\text{IC}}(pp \rightarrow ppH)}{dx_2} = \frac{32\pi P_{\text{IC}}(z)}{9B(s')(1-x_2)} \left| \int \frac{d^2k}{k^4} \alpha_s(k^2) \mathcal{F}(x, k^2) \int d^2r H^\dagger(\vec{r}) e^{-i\vec{k}\cdot\vec{r}/2} (1 - e^{i\vec{k}\cdot\vec{r}}) \Psi_{\bar{c}c}(\vec{r}) \right. \\ \left. \times \int d^2\rho \Phi_p^\dagger(\vec{\rho}) e^{-i\vec{k}\cdot\vec{\rho}/2} (1 - e^{i\vec{k}\cdot\vec{\rho}}) \Psi_{3q}(\vec{\rho}) \right|^2. \quad (13)$$

Here

$$z = [x_F^H + \sqrt{(x_F^H)^2 + 4M_H^2/s}]/2 \approx x_F^H \approx 1 - x_1 \\ = M_H^2/s(1 - x_2). \quad (14)$$

This relation receives sizable corrections only at very small Higgs Feynman $x_F^H \sim 2M_H/\sqrt{s}$. Notice that the expansion of the exponentials in Eq. (13) contains only odd powers of $\vec{k}\cdot\vec{r}$ and $\vec{k}\cdot\vec{\rho}$. This signals a change of orbital momentum of the quark configurations participating in the one-gluon exchange process. In order to obtain a nonzero result of the integration over \vec{r} , either the initial or the final $\bar{c}c$ wave function must contain a factor $\vec{\nabla}_r$, i.e. it must be a P wave. Since we assume that the Higgs is a scalar, its $\bar{c}c$ component must be in a P -wave state, while the primordial $\bar{c}c$ in the projectile IC state should be in an S wave. This is vice versa for the proton p_1 : the final $|3q\rangle$ system is in an S wave, but $\Psi_{3q}(\vec{\rho})$ must be a P wave.

Notice that both the scalar Higgs and χ states may be produced from the same IC component of the proton containing an S -wave $\bar{c}c$. However, the production of J/ψ , Y , Z^0 requires an IC component containing a P -wave $\bar{c}c$, which is presumably more suppressed.

The P -wave LC wave function of the Higgs in an impact parameter representation is given by the Fourier transform of its Breit-Wigner propagator:

$$H(\vec{r}) = i \frac{\sqrt{N_c} G_F}{2\pi} m_c \bar{\chi} \vec{\sigma} \chi \frac{\vec{r}}{r} \left[\epsilon Y_1(\epsilon r) - \frac{ir}{2} \Gamma_H M_H Y_0(\epsilon r) \right]. \quad (15)$$

Here G_F is the Fermi constant, χ and $\bar{\chi}$ are the spinors for c and \bar{c} , respectively, and

$$\epsilon^2 = \alpha(1 - \alpha)M_H^2 - m_c^2, \quad (16)$$

where α is the fraction of the LC momentum of the Higgs carried by the c quark. The functions $Y_{0,1}(x)$ in Eq. (15) are the second order Bessel functions and Γ_H is the total width of the Higgs. Assuming $\Gamma_G \ll M_H$, we neglect the second term in Eq. (15).

The LC wave function Eq. (16) assumes that the Higgs mass is much larger than the quark masses, which is

same value for q_L . In fact, analogous calculations performed in the dipole approach with the same form of the universal dipole cross section lead to very good agreement with data with no fitting parameter (see [42]).

Finally, combining all the above modifications and performing the p_1 integration in Eq. (5), we arrive at

probably true for charm and bottom. However, it is quite probable that for top-antitop in the Higgs $2m_t > M_H$, then the wave function is different,

$$H_t(\vec{r}) = \frac{\sqrt{N_c} G_F}{2\pi} m_t \bar{\chi} \vec{\sigma} \chi \frac{\vec{r}}{r} \epsilon_t K_1(\epsilon_t r), \quad (17)$$

where $K_1(x)$ is the modified Bessel function and

$$\epsilon_t^2 = m_t^2 - \alpha(1 - \alpha)M_H^2. \quad (18)$$

The probabilities computed from the wave functions, Eqs. (15) and (18), require regularization in the ultraviolet limit [43,44], as is the case of the $\bar{Q}q$ wave function of a transverse photon. Such wave functions are not solutions of the Schrödinger equation, but are distribution functions for perturbative fluctuations. They are overwhelmed by very heavy fluctuations with large intrinsic transverse momenta, or vanishing transverse separations. Such pointlike fluctuations lead to a divergent normalization, but they do not interact with external color fields, i.e., they are not observable. All the expressions for any measurable quantity, including the cross section, are finite.

As we have discussed, the IC wave function can be modeled as a nonperturbative 5 -quark stationary state $|3qc\bar{c}\rangle$, or as a perturbative fluctuation $|3q\rangle \rightarrow |3qc\bar{c}\rangle$. Correspondingly, the $\bar{c}c$ wave function within the Fock state will be assumed to be a linear combination of non-perturbative and perturbative distribution amplitudes,

$$\Psi_{\bar{c}c}(\vec{r}) = \beta \Psi_{\bar{c}c}^{\text{np}}(\vec{r}) + \sqrt{1 - \beta^2} \Psi_{\bar{c}c}^{\text{pt}}(\vec{r}). \quad (19)$$

The parameter β , which controls the relation between the nonperturbative and perturbative IC contributions, is such that $0 \leq \beta \leq 1$. The nonperturbative wave function should be an S -wave solution of the Schrödinger equation. Assuming an oscillator potential form we get

$$\Psi_{\bar{c}c}^{\text{np}}(\vec{r}) = \sqrt{\frac{m_c \omega}{2\pi}} \exp(-r^2 m_c \omega/4), \quad (20)$$

where ω is the oscillation frequency, as mentioned earlier.

Since the Higgs is produced from an S -wave $\bar{c}c$, the perturbative distribution amplitude is ultraviolet stable and can be normalized to 1, in order to correspond to P_c as a

probability to have such a charm quark pair in the proton

$$\Psi_{\bar{c}c}^{\text{pt}}(\vec{r}) = \frac{m_c}{\sqrt{\pi}} K_0(m_c r). \quad (21)$$

Here the modified Bessel function $K_0(m_c r)$ is the Fourier transform of the energy denominator associated with the $\bar{c}c$ fluctuation. We assume the c and \bar{c} quarks carry equal fractional momenta. For fixed α_s , the energy denominator governs the probability of the fluctuation in momentum space, since perturbatively one treats the charm quarks as free particles.

Now we can calculate the part of the matrix element in Eq. (13) related to Higgs production from the IC. We assume the initial $\bar{c}c$ wave function to be a linear combination (19) of the nonperturbative, Eq. (20), and perturbative, Eq. (21), wave functions, and the final-state wave function of the $\bar{c}c$ pair in the Higgs in the form (15). The result reads

$$\begin{aligned} & \int d^2 r H^\dagger(\vec{r}) e^{i\vec{k}\cdot\vec{r}/2} (1 - e^{-i\vec{k}\cdot\vec{r}}) \Psi_{\bar{c}c}(\vec{r}) \\ &= \frac{4}{\sqrt{\pi}} \frac{m_c^2}{M_H^2} \sqrt{N_c G_F \bar{\chi}} \vec{\sigma} \chi \vec{k} \left[\beta \sqrt{\frac{\omega}{2m_c}} \right. \\ & \quad \left. + \sqrt{1 - \beta^2} \ln\left(\frac{M_H}{2m_c}\right) \right]. \end{aligned} \quad (22)$$

Here we have made use of $M_H \gg m_c$ and expanded the exponentials $\exp(\pm i\vec{k}\cdot\vec{r})$ up to the first nonvanishing term. We also dropped the integration over α , assuming that the c and \bar{c} in the IC component carry the same momentum, i.e. $\Psi_{\bar{c}c}(r, \alpha) = \Psi_{\bar{c}c}(r) \delta(\alpha - 1/2)$. Correspondingly, we have fixed $\epsilon = M_H/2$ and we will assume $\beta \ll 1$.

The result of integration in Eq. (22) shows that the perturbative contribution is quite enhanced relative to the nonperturbative term. First of all, the enhancement by a

factor of $\sqrt{2m_c/\omega}$ is due to the fact that the projection to the pointlike Higgs wave function is proportional to $\Psi_{\bar{c}c}^{\text{IC}}(0)$, and the perturbative fluctuation has a smaller radius. Another enhancement factor, $\ln(M_H/2m_c)$, is due to the long power tail in the momentum distribution in the perturbative IC wave function, while the nonperturbative one has a Gaussian cut off. Thus, the perturbative term in the matrix element Eq. (22) is relatively enhanced by 1 order of magnitude.

Notice that the nonrelativistic nonperturbative solution should not be used for convolution with the highly perturbative Higgs wave function. The large transverse momentum tail of the IC should be represented by the perturbative term in Eq. (19). Unfortunately, the normalization of such a perturbative tail is unknown, and we normalize it to the IC weight of 1%.

Enhancement of the perturbative intrinsic heavy flavor in Higgs production is especially large for the top component. Using the IT wave function, Eq. (17), we get

$$\begin{aligned} & \int d^2 r H_{tt}^\dagger(\vec{r}) e^{i\vec{k}\cdot\vec{r}/2} (1 - e^{-i\vec{k}\cdot\vec{r}}) \Psi_{tt}^{\text{pt}}(\vec{r}) \\ &= \frac{1}{\sqrt{\pi}} \frac{m_t^2}{M_H^2} \sqrt{N_c G_F \bar{\chi}} \vec{\sigma} \chi \vec{k} \left[1 + \frac{1 - \delta}{\delta} \ln(1 - \delta) \right], \end{aligned} \quad (23)$$

where $\delta = M_H^2/4m_t^2$.

The proton is produced in a similar way from the P -wave $3q$ in the projectile IC component. The exponentials, however, should not be expanded, since the radius is not small. Therefore, using the relation

$$\int_0^{2\pi} d\phi \tilde{\rho} (e^{i\tilde{\rho}\cdot\vec{k}/2} - e^{-i\tilde{\rho}\cdot\vec{k}/2}) = 4\pi i \rho \frac{\vec{k}}{k} J_1(k\rho/2), \quad (24)$$

we get for the integral over $d^2\rho$ in Eq. (13)

$$\int d^2\rho \frac{1}{\sqrt{\pi} R_{3q}} \frac{\tilde{\rho}}{\rho} e^{-\rho^2/2R_{3q}^2} (e^{i\tilde{\rho}\cdot\vec{k}/2} - e^{-i\tilde{\rho}\cdot\vec{k}/2}) \frac{1}{\sqrt{\pi} R_p} e^{-\rho^2/2R_p^2} = i \frac{\sqrt{\pi}}{4} \frac{\mathcal{R}^3 \vec{k}}{R_p R_{3q}} e^{-y} [J_0(y) - J_1(y)], \quad (25)$$

where $\mathcal{R}^2 = 2R_p^2 R_{3q}^2 / (R_p^2 + R_{3q}^2)$ and $y = \mathcal{R}^2 k^2 / 32$. For further estimates we assume that $R_p = R_{3q}$, so $\mathcal{R} = R_p$. Since we assumed a meson-type quark-diquark structure for the proton, the mean separation $R_p^2 = 2\langle r_{\text{ch}}^2 \rangle_p / 3$. The transition proton form factor, $\exp(-k^2 \mathcal{R}^2 / 32)$, cuts off the integration over d^2k .

Now we are in a position to perform the last integration over \vec{k} in Eq. (13),

$$\begin{aligned} \frac{d\sigma^{\text{IC}}(pp \rightarrow ppH)}{dx_2} &= \frac{32}{\pi^2} \frac{G_F P_{\text{IC}}(z)}{1 - x_2} \frac{m_c^4}{M_H^4} \frac{[\sigma_{\text{tot}}^{\pi p}(s')]^2}{B(s') \langle r_{\text{ch}}^2 \rangle_p} \frac{\gamma^2(s')}{[2 + 2\gamma(s') + \gamma^2(s')]^3} \left[1 + \frac{\langle r_{\text{ch}}^2 \rangle_p}{16 \langle r_{\text{ch}}^2 \rangle_\pi} \frac{1}{\gamma(s')} \right]^2 \\ & \quad \times \left[\beta \sqrt{\frac{\omega}{2m_c}} + \sqrt{1 - \beta^2} \ln\left(\frac{M_H}{2m_c}\right) \right]^2, \end{aligned} \quad (26)$$

where $\gamma(s') = R_p^2 / 4R_0^2(s')$.

The cross section of Higgs production from the intrinsic bottom has the same form as Eq. (26), and we assume that the weight of intrinsic heavy flavor scales as $P_{\text{IQ}} = P_{\text{IC}} m_c^2 / m_Q^2$. However, as we found above, if the Higgs mass is restricted by $M_H^2 < 4m_t^2$, production from the intrinsic perturbative top component of the proton has the cross section

$$\frac{d\sigma^{\text{IT}}(pp \rightarrow ppH)}{dx_2} = \frac{8}{\pi^2} \frac{G_F P_{\text{IT}}(z)}{1-x_2} \frac{m_t^4}{M_H^4} \frac{[\sigma_{\text{tot}}^{\pi p}(s')]^2}{B(s') \langle r_{\text{ch}}^2 \rangle_p} \frac{\gamma^2(s')}{[2 + 2\gamma(s') + \gamma^2(s')]^3} \left[1 + \frac{\langle r_{\text{ch}}^2 \rangle_p}{16 \langle r_{\text{ch}}^2 \rangle_\pi} \frac{1}{\gamma(s')} \right]^2 \left[1 + \frac{1-\delta}{\delta} \ln(1-\delta) \right]^2. \quad (27)$$

B. Feynman x_F^H distribution of Higgs particles

The x_F^H distribution of the cross section, Eqs. (26) and (27), is related to the LC wave function $\Psi_{\text{IC}}(R, z)$ of the system $3q - \bar{c}c$, namely, to the function $P_{\text{IC}}(z)$ defined in Eq. (8). The momentum fraction z is related to $x_{1,2}$ and x_F^H by Eq. (14). The shape of $P_{\text{IC}}(z)$ strongly correlates with the origin of IC, a nonperturbative component of the proton wave function or a perturbative fluctuation.

1. Nonperturbative IC

In principle, one can construct a hadronic LC wave function by diagonalizing the LC Hamiltonian. Here we will use the method of Ref. [45] for the Lorentz boost of the wave function, which is supposed to be known in the hadron rest frame. The Lorentz boost generates higher particle number quantum fluctuations which are missed by this procedure; however, this method works well in known cases [46,47], and even provides a nice cancellation of large terms violating the Landau-Yang theorem [48].

We assume that the rest frame IC wave function has the oscillatory form (in momentum space)

$$\tilde{\Psi}_{\text{IC}}(\vec{Q}, z) = \sqrt{P_{\text{IC}}(z)} \left(\frac{1}{\pi\omega\mu} \right)^{3/4} \exp\left(-\frac{\vec{Q}^2}{2\omega\mu}\right). \quad (28)$$

Here ω stands for the oscillator frequency and $\mu = M_{\bar{c}c} M_{3q} / (M_{\bar{c}c} + M_{3q})$ is the reduced mass of the $\bar{c}c$ and $3q$ clusters. For further estimates we use $M_{\bar{c}c} = 3$ GeV and $M_{3q} = 1$ GeV, although the latter could be heavier, since it is the P wave.

To express the 3-vector \vec{Q} by the effective mass of the system, $M_{\text{eff}} = \sqrt{\vec{Q}^2 + M_{\bar{c}c}^2} + \sqrt{\vec{Q}^2 + M_{3q}^2}$, one can switch to the LC variables, \vec{Q} and z ,

$$M_{\text{eff}}^2 = \frac{Q^2}{z(1-z)} + \frac{M_{\bar{c}c}^2}{z} + \frac{M_{3q}^2}{1-z}. \quad (29)$$

Then the longitudinal component Q_L in the exponent in (28) reads

$$Q_L^2 = \frac{M_{\text{eff}}^2}{4} + \frac{(M_{\bar{c}c}^2 - M_{3q}^2)^2}{4M_{\text{eff}}^2} - \frac{M_{\bar{c}c}^2 + M_{3q}^2}{2} - Q^2, \quad (30)$$

and the LC wave function acquires the form

$$\Psi_{\text{IC}}(Q, z) = K \sqrt{P_{\text{IC}}(z)} \exp\left\{ -\frac{1}{8\omega\mu} \left[M_{\text{eff}}^2 + \frac{(M_{\bar{c}c}^2 - M_{3q}^2)^2}{M_{\text{eff}}^2} \right] \right\}, \quad (31)$$

where

$$K^2 = \frac{1}{8Q_L} \left(\frac{1}{\pi\omega\mu} \right)^{3/2} \exp\left(\frac{M_{\bar{c}c}^2 + M_{3q}^2}{2\omega\mu}\right) \left[1 - \frac{(M_{\bar{c}c}^2 - M_{3q}^2)}{M_{\text{eff}}^4} \right] \times \left[\frac{Q^2(2z-1)}{z^2(1-z)^2} - \frac{M_{\bar{c}c}^2}{z^2} + \frac{M_{3q}^2}{(1-z)^2} \right]. \quad (32)$$

Now we can calculate the z dependence of the function $P_{\text{IC}}(z)$ defined in Eq. (8), which controls the x_1 dependence of the cross section,

$$\frac{P_{\text{IC}}(z)}{P_{\text{IC}}} = \frac{1}{\sigma^{\text{IC}}(pp \rightarrow ppH)} \frac{d\sigma^{\text{IC}}(pp \rightarrow ppH)}{dx_1} = \frac{1}{P_{\text{IC}}} \int d^2Q |\Psi_{\text{IC}}(Q, z)|^2. \quad (33)$$

This function is plotted in Fig. 3. The distribution sharply peaks at $z \approx 0.75$, as one could expect, since the IC pair is heavy and should carry the main fraction of the proton momentum. Note that at high energies, in particular, at LHC, the momentum fraction z coincides with the Feynman x_H of the Higgs particle, with a high accuracy $\sim M_H^2/s$.

2. Perturbative intrinsic heavy flavors

The light-cone wave function of a perturbative fluctuation $p \rightarrow |3q\bar{Q}Q\rangle$ in momentum representation is controlled by the energy denominator,

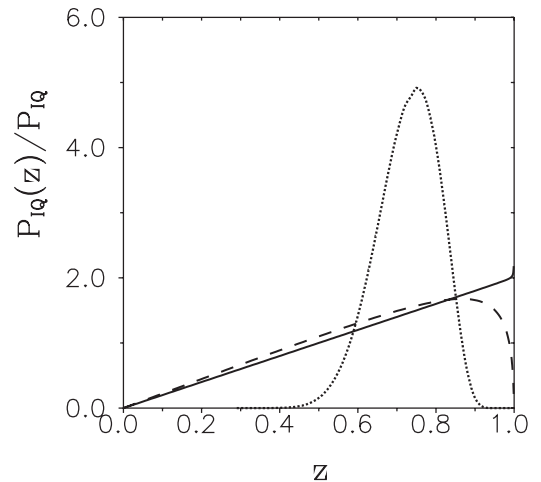


FIG. 3. The distribution of produced Higgs particles over the fraction of the proton beam momentum. The dotted, dashed, and solid curves correspond to Higgs production from nonperturbative IC ($\beta = 1$), perturbative IC ($\beta = 0$), and IT, respectively.

$$\Psi_{\text{IQ}}(Q, z, \kappa) \propto \frac{z(1-z)}{Q^2 + z^2 m_p^2 + M_{\bar{Q}Q}^2(1-z)}. \quad (34)$$

Momentum \vec{Q} was defined in Fig. 2 and Eq. (5). The effective mass of the $\bar{Q}Q$ depends on the intrinsic transverse momentum of the $\bar{Q}Q$ pair, $M_{\bar{Q}Q}^2 = 4(\kappa^2 + m_Q^2)$. It is controlled by the convolution of the IC $\bar{Q}Q$ wave function with the P -wave $\bar{Q}Q$ wave function in the Higgs and the one-gluon exchange amplitude (see Fig. 2), which has the form

$$\int_0^\infty d\kappa^2 \Psi_{\text{IQ}}(Q, z, \kappa) [H_{\bar{Q}Q}(\vec{\kappa} + \vec{k}/2) - H_{\bar{Q}Q}(\vec{\kappa} - \vec{k}/2)] \\ \propto z(1-z) \frac{\ln\left[\frac{|M_H^2 - 4m_Q^2|(1-z)}{Q^2 + 4m_Q^2(1-z) + m_p^2 z^2}\right]}{M_H^2(1-z) + Q^2 + m_p^2 z^2}. \quad (35)$$

This expression peaks at $1-z \sim m_p/M_H$, therefore the logarithmic factor hardly varies as a function of Q^2 which is restricted by the proton form factor. Making use of this we perform integration in Eq. (33) and arrive at the following z distribution,

$$\sigma^{\text{IC}}(pp \rightarrow ppH) = \frac{32}{\pi^2} \frac{G_F P_{\text{IC}}}{z_0} \frac{m_c^4}{M_H^4} \frac{[\sigma_{\text{tot}}^{\pi p}(\tilde{s})]^2}{B(\tilde{s}) \langle r_{\text{ch}}^2 \rangle_p} \frac{\gamma^2(\tilde{s})}{[2 + 2\gamma(\tilde{s}) + \gamma^2(\tilde{s})]^3} \left[1 + \frac{\langle r_{\text{ch}}^2 \rangle_p}{16 \langle r_{\text{ch}}^2 \rangle_\pi} \frac{1}{\gamma(\tilde{s})}\right]^2 \\ \times \left[\beta \sqrt{\frac{\omega}{2m_c}} + \sqrt{(1-\beta^2)} \ln\left(\frac{M_H}{2m_c}\right) \right]^2, \quad (37)$$

where $\tilde{s} = s z_0 M_0^2 / M_H^2$. An analogous expression should be valid for Higgs production from intrinsic bottom. For top quark in the proton we use Eq. (27) which leads to

$$\sigma^{\text{IT}}(pp \rightarrow ppH) = \frac{8}{\pi^2} \frac{G_F P_{\text{IT}}}{z_0} \frac{m_t^4}{M_H^4} \frac{[\sigma_{\text{tot}}^{\pi p}(\tilde{s})]^2}{B(\tilde{s}) \langle r_{\text{ch}}^2 \rangle_p} \frac{\gamma^2(\tilde{s})}{[2 + 2\gamma(\tilde{s}) + \gamma^2(\tilde{s})]^3} \left[1 + \frac{\langle r_{\text{ch}}^2 \rangle_p}{16 \langle r_{\text{ch}}^2 \rangle_\pi} \frac{1}{\gamma(\tilde{s})}\right]^2 \left[1 + \frac{1-\delta}{\delta} \ln(1-\delta)\right]^2. \quad (38)$$

Notice that function $\gamma(\tilde{s})$ increases with energy as $\tilde{s}^{0.28}$, and such a steep rise of the denominator in Eq. (37) is not compensated by the rise of the total cross section in the numerator. Therefore, the diffractive cross sections, Eqs. (37) and (38), turn out to decrease at asymptotic energies approximately as inverse energy. This unexpected result may be interpreted as follows. The source of the falling energy dependence is the steep rise with energy of the mean transverse momentum of gluons as is given by the unintegrated gluon density, Eq. (11), $\langle k^2 \rangle = 4/R_0^2(x) \propto (s/M_H^2)^{0.28}$. Also, the integral over k^2 of the distribution (11) rises with energy, and its value at $k=0$ is steeply falling. The rise comes for large transverse momenta which, however, are cut off by the nucleon form factor, Eq. (20). This is why the diffractive cross section (37) is steeply falling. Indeed, without this form factor, for instance in the reaction $pp \rightarrow HXp$, the cross section would rise as $(s/M_H)^{0.7}$.

$$\frac{P_{\text{IQ}}(z)}{P_{\text{IQ}}} = Nz(1-z) \frac{\left\{ \ln\left[\frac{|M_H^2 - 4m_Q^2|(1-z)}{4m_Q^2(1-z) + m_p^2 z^2}\right] \right\}^2}{M_H^2(1-z) + m_p^2 z^2}, \quad (36)$$

where N is a constant normalizing to 1 the integral over z . The corresponding z distributions for charm and top are shown in Fig. 3 by dotted (dashed) and solid curves, respectively.

C. Energy dependence

One can integrate in Eqs. (26) and (27) over x_2 using relation (14). Since the momentum distribution of Higgs produced from the nonperturbative IC sharply peaks at $z = z_0 = 0.75$, one can replace $P_{\text{IC}}(z) \Rightarrow \delta(z - z_0)P_{\text{IC}}$. With a reasonable accuracy we can fix z at the same value for the perturbative case and heavier flavors too, which is justified by the rather mild dependence on s' of other factors in Eqs. (26) and (27).

Since at high energies $z \approx x_H \approx 1 - x_1$, performing integration in Eq. (26) one arrives at

Nevertheless, at the energy of LHC, $\sqrt{s} = 14$ TeV, the effective energy is rather low, $\sqrt{\epsilon}s = 120$ GeV (we assume $M_H = 100$ GeV) and the cross section still rises with energy. Indeed, $R_0^2 = 0.36$ fm², so $\gamma(\epsilon s) = 0.55$ is still rather small at this energy, and the cross sections, Eqs. (37) and (38), rise as

$$\sigma^{\text{IQ}}(pp \rightarrow ppH)_{\text{LHC}} \propto \left(\frac{s}{M_H^2}\right)^{0.6}. \quad (39)$$

However, at much higher energies the energy dependence will switch to a steeply falling one. Besides, absorptive or unitarity corrections are known to slow down the rise of the cross sections.

D. Absorptive corrections

The amplitude of any off-diagonal large rapidity gap process is subject to unitarity or absorptive corrections,

which have the intuitive meaning of a survival probability of the participating hadrons. To include these corrections one should replace the diffractive amplitude as

$$f_{sd}^{pp}(b, s) \Rightarrow f_{sd}^{pp}(b, s)[1 - \text{Im}f_{\text{el}}^{pp}(b, s)]. \quad (40)$$

The data for elastic pp scattering show that the partial amplitude $f_{\text{el}}^{pp}(b, s)$ is independent of energy at small impact parameters $b \rightarrow 0$, while rising as a function of energy at large b [49–51]. This is usually interpreted as a manifestation of saturation of the unitarity limit, $\text{Im}f_{\text{el}}^{pp} \leq 1$. Indeed, this condition imposes a tight restriction at small b , where $\text{Im}f_{\text{el}}^{pp} \approx 1$, leaving almost no room for further rise. We will treat the Pomeron as a Regge pole without unitarity corrections:

$$\tilde{\sigma}^{\text{IQ}}(pp \rightarrow ppH) = \sigma^{\text{IQ}}(pp \rightarrow ppH) \left\{ 1 - \frac{1}{\pi} \frac{\sigma_{\text{tot}}^{pp}(s')}{B(s') + 2B_{\text{el}}^{pp}(s')} + \frac{1}{(4\pi)^2} \frac{[\sigma_{\text{tot}}^{pp}(s')]^2}{B_{\text{el}}^{pp}(s')[B(s') + B_{\text{el}}^{pp}(s')]} \right\}. \quad (42)$$

This is not a severe suppression even at the energy of LHC, where the absorptive factor is 0.2.

Including the absorptive corrections we calculated the total cross sections for diffractive Higgs production, $pp \rightarrow Hpp$, from the intrinsic heavy quark (IQ) components. The results at the energy of LHC, $\sqrt{s} = 14$ TeV, are plotted as a function of Higgs mass in Fig. 4. We assume a perturbative origin for all intrinsic components, a $1/m_Q^2$ scaling for their weights, and a 1% probability of IC for $\beta = 0$ in Eq. (37). Note that the contributions of the intrinsic charm and bottom fall steeply with the mass of the Higgs in accordance with Eq. (37). The contribution of the intrinsic top rises with M_H unless $M_H > 2m_t \approx 350$ GeV; then the cross section starts falling.

In our case, the enhanced corrections (also called Gribov's corrections) increase, rather than suppress the

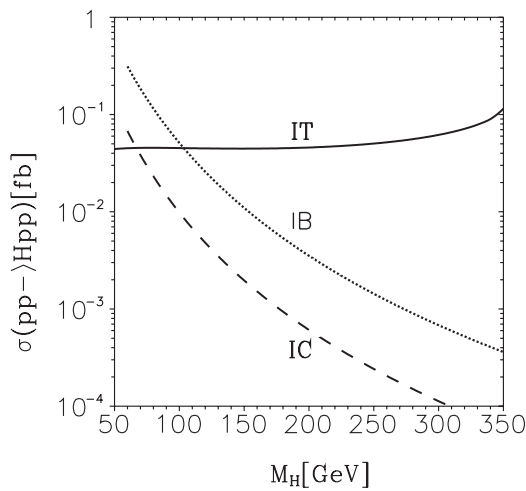


FIG. 4. The cross section of the reaction $pp \rightarrow Hp + p$ as a function of the Higgs mass. Contributions of IC (dashed line), IB (dotted line), and IT (solid line).

$$\text{Im}f_{\text{el}}^{pp}(b, s) = \frac{\sigma_{\text{tot}}^{pp}(s)}{4\pi B_{\text{el}}^{pp}(s)} \exp\left[-\frac{b^2}{2B_{\text{el}}^{pp}(s)}\right], \quad (41)$$

where $\sigma_{\text{tot}}^{pp}(s) = 21.8 \text{ mb} \times (s/M_0^2)^\epsilon$, and $\epsilon = 0.08$; $B_{\text{el}}^{pp}(s) = B_{\text{el}}^0 + 2\alpha'_p \ln(s/M_0^2)$ with $B_{\text{el}}^0 = 7.5 \text{ GeV}^{-2}$. Because of the accidental closeness of $2\alpha'_p/B_{\text{el}}^0 = 0.067$ and ϵ , the preexponential factor in (41) hardly changes with energy even without unitarity corrections. It is demonstrated in Ref. [51] that not only at $b = 0$, but in the whole range of impact parameters, the model, Eq. (41), describes correctly the energy dependence of the partial amplitude $f_{\text{el}}^{pp}(b, s)$.

Thus we arrive at the absorption corrected cross section,

survival probability. In Regge models one can check this by applying the quasieikonal model which leads to a “gray disk” rather than “black disk” regime in the Froissart limit. It is more correct to rely on the dipole approach. For each Fock state the survival probability $\langle \exp[-\sigma(r)T(b)] \rangle$ is larger than the eikonal one, $\exp[-\langle \sigma(r) \rangle T(b)]$, where $T(b)$ is the thickness function at impact parameter \vec{b} (profile function of the target), and $\sigma(r)$ is the dipole cross section. To be on the safe side we use the latter more conservative estimate. The difference between these two approaches is not dramatic, even for nuclei (see Ref. [31]).

V. FURTHER POSSIBILITIES TO GET A LARGER CROSS SECTION

A. Direct production of Higgs from a colorless IQ

A heavy flavor $\bar{Q}Q$ pair in the IQ component of the proton may be found in a colorless state. In this case the Higgs particle can be produced directly from this pair via Pomeron exchange as is shown in Fig. 5. We consider the

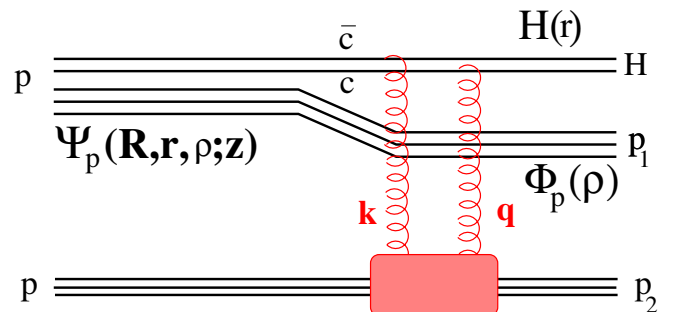


FIG. 5 (color online). Higgs production via Pomeron exchange.

example of intrinsic charm of a nonperturbative origin throughout this section.¹

At first glance one may think that this channel is less suppressed by powers of the Higgs mass compared to the mechanism presented in Fig. 2. Indeed, the integration over \vec{k} does not have the upper cutoff imposed by the proton form factor in the previous case; therefore it may compensate two powers of M_H in the amplitude. This analysis is correct. Nevertheless the amplitude turns out to be more suppressed than in Fig. 2.

The diffractive amplitude $A(x_2, \vec{p}_1, \vec{p}_2)$ is proportional to the matrix element of the dipole cross section $\sigma_{\bar{q}q}(r)$ between the initial $\bar{c}c$ wave function $\Psi_{\bar{c}c}(r)$ and the distribution amplitude of the $\bar{c}c$ in the Higgs,

$$A(x_2, \vec{p}_1, \vec{p}_2) \propto \int d^2r H^\dagger(\vec{r}) \sigma_{\bar{q}q}(r) \Psi_{\bar{c}c}(r). \quad (43)$$

This factor contains all the dependence on the Higgs mass. To estimate it one can use a Gaussian shape for both $\Psi_{\bar{c}c}(r)$ and $H(\vec{r})$. Then one finds $A \propto \sqrt{m_c \omega} / M_H^3$. A more refined calculation confirms this,

$$\begin{aligned} \int d^2r H^\dagger(\vec{r}) \sigma_{\bar{q}q}(r) \Psi_{\bar{c}c}(r) &= \frac{3\sigma_0(s) \sqrt{2\pi N_c G_F}}{2m_c \omega R_0^2(s)} \\ &\times U\left(\frac{3}{2}, 0, \frac{M_H^2}{4m_c \omega}\right) \\ &= \frac{12\sigma_0(s)}{R_0^2(s)} \sqrt{2\pi N_c G_F} \frac{\sqrt{m_c \omega}}{M_H^3}, \end{aligned} \quad (44)$$

where the initial state $\bar{c}c$ pair is assumed to be in a P wave. Here $U(a, b, x)$ is the confluent hypergeometric function, and we use its asymptotic behavior at $x \gg 1$,

$$U(a, b, x) = x^{-a} + O(x^{-a-1}). \quad (45)$$

Notice that a convolution similar to Eq. (43) also defines the scale dependence of the amplitude of photoproduction of heavy quarkonia, which also behaves like $(Q^2 + M^2)^{-3}$. Thus, the complementary mechanism of diffractive Higgs production, besides the smaller probability to find the colorless IC component, is additionally suppressed by $1/M_H^2$ compared to the dominant mechanism depicted in Fig. 2. Therefore, this contribution can be safely neglected.

¹Here we only consider the nonperturbative colorless IQ component, since the colorless perturbative contribution is suppressed in the heavy quark limit. The dominant contribution to IQ is in a color octet configuration which corresponds to the insertion of the $G_{\mu\nu}^3/m_Q^2$ effective operator. The color singlet IQ comes from the effective operator G^4/m_H^4 , as in the Euler Heisenberg QED Lagrangian, so it is power suppressed in the IQ distribution.

B. Nuclear enhancement

The produced Higgs is supposed to escape detection and to be identified only by using the missing mass spectrum. One may also consider the same reaction on a bound proton in pA collisions where the nuclear debris spectators fly in the same direction as the Higgs. The nuclear enhancement in this case is not as large as one could naively expect. The reason is that absorptive corrections are stronger than those considered above in Sec. IV D for the case of pp collisions. The survival probability represented by the last factor in Eq. (42) can be evaluated within the Glauber approximation for pA collisions as

$$Z_{\text{eff}} = \frac{Z}{A} \int d^2b T_A(b) e^{-\sigma_{\text{in}}^{pp} T_A(b)}, \quad (46)$$

where $T_A(b) = \int_{-\infty}^{\infty} dz \rho_A(b, z)$ is the nuclear thickness function at impact parameter \vec{b} , and $\rho_A(b)$ is the nuclear density. We assume here that diffractive recoil neutrons cannot be detected; otherwise the factor (46) should be multiplied by A/Z .

The nuclear enhancement for lead, according to (46), is rather mild, of about an order of magnitude, since $Z_{\text{eff}} \approx 2.5$ should be compared with the suppression factor 0.2, for pp collisions calculated in Sec. IV D. Gribov corrections [52] are known to make nuclei more transparent, therefore they may substantially increase the survival probability factor [31,53]. If we employ the simplest quadratic dependence of the dipole cross section $\sigma_{\bar{q}q}(r) \propto r^2$, then the nuclear enhancement is considerably larger, a factor of about 50.

VI. CONCLUSIONS

The key assumption underlying our analysis of high x_F Higgs hadroproduction is the presence of intrinsic heavy flavor $|uudQ\bar{Q}\rangle$ Fock components in the proton bound-state wave function. Such quantum fluctuations are, in fact, rigorous consequences of QCD. The probability for intrinsic heavy quarks on the heavy quark mass falls as $\Lambda_{\text{QCD}}^2/M_Q^2$ in non-Abelian theories and can be computed from the operator product expansion [11]. In such Fock states the heavy quarks Q and \bar{Q} carry the highest light-cone momentum fractions. Thus, although they have small probability, intrinsic heavy quark Fock states are highly efficient in transferring the momentum of the proton to the momenta of particles in the final state, especially heavy quarkonium and the Higgs which can sum the momenta of both the Q and \bar{Q} . It is thus interesting and important that measurements of the production of heavy quarkonium at high x_F as well as other heavy hadrons such as the Λ_b and Λ_c be carried out at RHIC and the Tevatron, as well as the LHC in order to test this novel feature of QCD.

As we have reviewed in Sec. III, there is substantial but not conclusive phenomenological evidence for intrinsic charm at the 1% probability level in the proton. It is thus

particularly important to have measurements of the charm and bottom structure functions in deep inelastic lepton-proton scattering over the full range of x_{Bj} . One must allow for intrinsic sea components at any scale Q_0 when parametrizing the proton's structure functions, since the intrinsic Fock states are responsible for the $\bar{u}(x) \neq \bar{d}(x)$, $s(x) \neq \bar{s}(x)$ asymmetries, as well as the high- x $c(x)$ and $b(x)$ distributions. There are also important nuclear and heavy quark threshold effects related to intrinsic charm which can be tested at lower energy fixed-target facilities such as JLAB, GSI-FAIR, and J-PARC [54].

As we have emphasized here, the materialization of intrinsic heavy flavor states in the proton leads to Higgs production in the proton fragmentation region: this includes inclusive production $pp \rightarrow HX$, singly diffractive production $pp \rightarrow p + HX$, and exclusive diffractive production $pp \rightarrow p + H + p$, reactions which should be considered in addition to the conventional central rapidity production processes. The fractional momentum distribution for a Higgs produced by combining the momenta of both heavy quarks in the IQ Fock states is presented in Fig. 3. As seen in the figure, the Higgs can be produced with momentum fractions as large as $x_F \sim 0.8$ or even higher. One can also produce the Higgs inclusively from leading-twist perturbative QCD processes such as $gc \rightarrow Hc$ and $gb \rightarrow Hb$ where the high momentum of one intrinsic heavy quark is transferred to the Higgs.

The large background from the inclusive process $pp \rightarrow [b\bar{b}]X$ can be dramatically suppressed by triggering on diffractively produced high p_T dijets which balance closely in transverse momentum, corresponding to the signal from Higgs decay. The probability of forward diffractive dijet production is known to fall steeply as a function of the dijet effective mass, $d\sigma/dp_T^2 \propto M_{q\bar{q}}^{-8}$ [55]. In our case, since the dijet is produced from IQ via one-gluon exchange, the falloff is less steep, $d\sigma/dp_T^2 \propto M_{q\bar{q}}^{-6}$. This can be derived from the convolution equation (22), replacing the Higgs wave function $H(r)$ by a plane wave $\exp(i\vec{p}_T \vec{r})$, where $p_T \approx M_H/2$. This four-orders-of-magnitude suppression of the background nearly compensates for the small factor G_F in the Higgs channel. If the Higgs mass exceeds 200 GeV, the background from the charm and beauty dijets should be even smaller than the Higgs signal. Notice that such a strong suppression of the background in high p_T dijet events is specific for single

diffractive production and may be considered as an advantage.

In this paper, we have focused on diffractive exclusive Higgs production $pp \rightarrow p + H + p$, since, in principle, only the final-state protons need to be measured and the Higgs can be reconstructed from the missing mass distribution. We note, however, that detecting the diffractive signal $pp \rightarrow p + H + p$ poses new challenges: When the Higgs is produced at large x_F , one of the final-state protons will need to be detected at a small momentum fraction $\sim 1 - x_F$, which is outside of the usual acceptance of forward proton detectors.

The underlying color structure of the intrinsic Fock state and the gauge theory properties of the two-gluon exchange mechanism for high energy diffraction play key roles in the physics of the exclusive diffractive Higgs hadroproduction process. The main result of our analysis, the cross sections given in Eqs. (37) and (38), demonstrates that the heavier the intrinsic heavy quark, the larger the cross section for the doubly diffractive reaction. It rises with m_Q linearly if the heavy quarks are confined by a potential, and is presented in Fig. 4 if the $\bar{Q}Q$ appear in the proton as a perturbative fluctuation. The production cross section also steeply rises with energy $\propto s^{0.7}$, which is characteristic for the energy dependence of hard reactions. Absorptive corrections slow down this rise and eventually stop it at very high energies, above the energy range of LHC. Asymptotically, in the Froissart regime, this cross section is expected to fall. Numerical predictions for diffractive Higgs production from IC, IB, and IT components are shown in Fig. 4. The cross section will be further enhanced from possible Fock states of the proton containing supersymmetric partners of quarks or gluons. We have also discussed a potential increase in the rate for such reactions using proton-nucleus collisions.

ACKNOWLEDGMENTS

This work was supported in part by the Department of Energy under Contract No. DE-AC02-76SF00515, by Fondecyt (Chile) Grant No. 1030355 and No. 1050519, by DFG (Germany) Grant No. PI182/3-1, and by the cooperation program Ecos-Conicyt C04E04 between France and Chile. We are thankful to Fred Goldhaber, Paul Hoyer, and Alexander Tarasov for informative and helpful discussions.

-
- [1] S. J. Brodsky, C. Peterson, and N. Sakai, *Phys. Rev. D* **23**, 2745 (1981).
 [2] S. J. Brodsky, P. Hoyer, C. Peterson, and N. Sakai, *Phys. Lett. B* **93**, 451 (1980).
 [3] J. Pumplin, hep-ph/0508184.

- [4] H. P. Nilles, *Phys. Rep.* **110**, 1 (1984).
 [5] A. De Roeck, V. A. Khoze, A. D. Martin, R. Orava, and M. G. Ryskin, *Eur. Phys. J. C* **25**, 391 (2002), and references therein.
 [6] M. Deile (TOTEM Collaboration), hep-ex/0410084.

- [7] C. T. Munger, S. J. Brodsky, and I. Schmidt, *Phys. Rev. D* **49**, 3228 (1994).
- [8] G. Baur *et al.*, *Phys. Lett. B* **368**, 251 (1996).
- [9] G. Blanford, D.C. Christian, K. Gollwitzer, M. Mandelkern, C. T. Munger, J. Schultz, and G. Zioulas (E862 Collaboration), *Phys. Rev. Lett.* **80**, 3037 (1998).
- [10] For a review of the light-front formalism, see S. J. Brodsky, H. C. Pauli, and S. S. Pinsky, *Phys. Rep.* **301**, 299 (1998).
- [11] M. Franz, V. Polyakov, and K. Goetze, *Phys. Rev. D* **62**, 074024 (2000); see also S. J. Brodsky, J. C. Collins, S. D. Ellis, J. F. Gunion, and A. H. Mueller, in Proceedings of 1984 Summer Study on the SSC, Snowmass, CO, 1984, Report No. DOE/ER/40048-21 P4.
- [12] S. J. Brodsky and S. Gardner, *Phys. Rev. D* **65**, 054016 (2002).
- [13] S. J. Brodsky and M. Karliner, *Phys. Rev. Lett.* **78**, 4682 (1997).
- [14] J. S. Kosmas, S. Kovalenko, and I. Schmidt, *Phys. Lett. B* **519**, 78 (2001).
- [15] J. J. Aubert *et al.* (European Muon Collaboration), *Nucl. Phys.* **B213**, 31 (1983).
- [16] B. W. Harris, J. Smith, and R. Vogt, *Nucl. Phys.* **B461**, 181 (1996).
- [17] J. Badier *et al.* (NA3 Collaboration), *Z. Phys. C* **20**, 101 (1983).
- [18] M. J. Leitch *et al.* (FNAL E866/NuSea Collaboration), *Phys. Rev. Lett.* **84**, 3256 (2000).
- [19] S. J. Brodsky and P. Hoyer, *Phys. Rev. Lett.* **63**, 1566 (1989).
- [20] P. Hoyer, M. Vanttinen, and U. Sukhatme, *Phys. Lett. B* **246**, 217 (1990).
- [21] S. J. Brodsky, P. Hoyer, A. H. Mueller, and W. K. Tang, *Nucl. Phys.* **B369**, 519 (1992).
- [22] B. Z. Kopeliovich, J. Nemchik, I. K. Potashnikova, M. B. Johnson, and I. Schmidt, *Phys. Rev. C* **72**, 054606 (2005).
- [23] V. D. Barger, F. Halzen, and W. Y. Keung, *Phys. Rev. D* **25**, 112 (1982).
- [24] R. Vogt and S. J. Brodsky, *Nucl. Phys.* **B478**, 311 (1996).
- [25] P. Chauvat *et al.*, *Phys. Lett. B* **199**, 304 (1987); see also the analysis of J. F. Gunion and R. Vogt, hep-ph/9706252.
- [26] E. M. Aitala *et al.* (E791 Collaboration), *Phys. Lett. B* **495**, 42 (2000).
- [27] E. M. Aitala *et al.* (Fermilab E791 Collaboration), *Phys. Lett. B* **539**, 218 (2002).
- [28] K. L. Giboni *et al.*, *Phys. Lett. B* **85**, 437 (1979).
- [29] M. H. L. Wang *et al.*, *Phys. Rev. Lett.* **87**, 082002 (2001).
- [30] K. Kodama *et al.*, *Phys. Lett. B* **316**, 188 (1993).
- [31] B. Z. Kopeliovich, I. K. Potashnikova, and I. Schmidt, *Phys. Rev. C* **73**, 034901 (2006).
- [32] B. Z. Kopeliovich, A. Schäfer, and A. V. Tarasov, *Phys. Rev. D* **62**, 054022 (2000).
- [33] M. Basile *et al.*, *Nuovo Cimento Soc. Ital. Fis. A* **65**, 408 (1981); G. Bari *et al.*, *Nuovo Cimento Soc. Ital. Fis. A* **104**, 1787 (1991).
- [34] R. Vogt and S. J. Brodsky, *Phys. Lett. B* **349**, 569 (1995).
- [35] J. Badier *et al.* (NA3 Collaboration), *Phys. Lett. B* **114**, 457 (1982).
- [36] A. Ocherashvili *et al.* (SELEX Collaboration), *Phys. Lett. B* **628**, 18 (2005).
- [37] B. Z. Kopeliovich, L. I. Lapidus, and A. B. Zamolodchikov, *Sov. Phys. JETP* **33**, 612 (1981).
- [38] M. Burkardt and B. Warr, *Phys. Rev. D* **45**, 958 (1992).
- [39] S. J. Brodsky and B. Q. Ma, *Phys. Lett. B* **381**, 317 (1996).
- [40] M. L. Good and W. D. Walker, *Phys. Rev.* **120**, 1857 (1960); B. Z. Kopeliovich, I. K. Potashnikova, and Ivan Schmidt, in Proceedings of the 1st Latin American Workshop on High Energy Phenomenology, Porto Alegre, Brazil, 2005, hep-ph/0604097.
- [41] K. Golec-Biernat and M. Wüsthoff, *Phys. Rev. D* **59**, 014017 (1999).
- [42] Yu. Ivanov *et al.*, *Phys. Rev. D* **62**, 094022 (2000).
- [43] B. Z. Kopeliovich, J. Raufeisen, and A. V. Tarasov, *Phys. Rev. C* **62**, 035204 (2000).
- [44] M. B. Johnson *et al.*, *Phys. Rev. Lett.* **86**, 4483 (2001); *Phys. Rev. C* **65**, 025203 (2002).
- [45] M. V. Terent'ev, *Sov. J. Nucl. Phys.* **24**, 106 (1976).
- [46] J. Hüfner, Yu. P. Ivanov, B. Z. Kopeliovich, and A. V. Tarasov, *Phys. Rev. D* **62**, 094022 (2000).
- [47] B. Z. Kopeliovich, A. V. Tarasov, J. Hüfner, *Nucl. Phys.* **A696**, 669 (2001).
- [48] B. Z. Kopeliovich and A. V. Tarasov, *Nucl. Phys.* **A710**, 180 (2002).
- [49] U. Amaldi and K. R. Schubert, *Nucl. Phys.* **B166**, 301 (1980).
- [50] B. Z. Kopeliovich, B. Povh, and E. Predazzi, *Phys. Lett. B* **405**, 361 (1997).
- [51] B. Z. Kopeliovich, I. K. Potashnikova, B. Povh, and E. Predazzi, *Phys. Rev. Lett.* **85**, 507 (2000); *Phys. Rev. D* **63**, 054001 (2001).
- [52] V. N. Gribov, *Sov. Phys. JETP* **56**, 892 (1968).
- [53] B. Z. Kopeliovich, *Phys. Rev. C* **68**, 044906 (2003).
- [54] For a survey of such tests, see S. J. Brodsky, hep-ph/0411046.
- [55] V. M. Braun, D. Yu. Ivanov, A. Schäfer, and L. Szymanowski, *Nucl. Phys.* **B638**, 111 (2002).